

## Carbon utilization in the Eurasian sector of the Arctic Ocean

Kristina Olsson<sup>1</sup> and Leif G. Anderson

Department of Analytical and Marine Chemistry, Göteborg University, Göteborg, Sweden.

Markus Frank

Institut für Umweltphysik der Universität Heidelberg, Heidelberg, Germany.

Anna Luchetta

Instituto Talassographico di Trieste, Trieste, Italy

William Smethie

Lamont-Doherty Earth Observatory, New York 10964, New York

### Abstract

Production and remineralization of carbon in the Eurasian sector have been estimated based on a combined data set of the *Oden—91* and *Polarstern—93* (ARK IX—4) expeditions. This sector includes the deep Nansen and Amundsen Basins and their linked shelf seas, i.e., the Barents, Kara, and Laptev Seas. The water masses in this region are composed of Atlantic water, river runoff, and sea ice-melt water. The fractionation between these source waters is elucidated from the  $\delta^{18}\text{O}$ –salinity relation and conservation of mass. By combining preformed nitrate concentrations of the source waters with the fractionation model and the measured nitrate concentrations, nitrate deficits and excesses are calculated. These concentrations are then converted to carbon equivalents by applying a C/N ratio, whereby a measure of apparent carbon utilization (ACU) is obtained. From the relative inventory of ACU along the slope and deep basin sections, we conclude that the shelf areas are the dominant productivity sites and that the productivity signal is transported to all water masses in the Eurasian Basin. The flux of utilized carbon from the Barents–Kara and Laptev Seas is about 0.022 Gton C yr<sup>-1</sup>.

The Arctic Ocean was once regarded as the most oligotrophic of oceans (e.g., Platt and Subba Rao 1975) due to extensive ice cover, low solar angle, and temperatures but is now considered as a potentially important site of carbon dioxide fixation (Wheeler et al. 1996). The marginal ice zones (MIZ) in particular, including polynyas, offer conditions that enhance photosynthetic activity (e.g., Alexander and Niebauer 1981; Rey and Loeng 1985; Sakshaug and Skjoldal 1989), especially if there is advection of nutrient-rich water into the MIZ area (Wallace et al. 1995).

The magnitude and extent of ice algal production is under current debate. A general consensus of the perennial ice cover inhibiting primary production prevails (e.g., Subba

Rao and Platt 1984; Dunbar 1981; Sakshaug and Skjoldal 1989) even though high ice algal production in the sea ice realm is observed, at least on shorter time scales (Horner 1990).

The Chukchi and East Siberian seas are thought to be the most productive areas of the Arctic Ocean, with reported areal productivity in local regions of 480 g C m<sup>-2</sup> yr<sup>-1</sup> (Springer and McRoy 1993). These high figures are essentially a result of the large nutrient supply through the Bering Strait. Total production estimates for the Barents Sea are lower, with model estimates of 40–90 g C m<sup>-2</sup> yr<sup>-1</sup> (Slagstad and Wassman 1996), as this shelf sea is fed by inflowing North Atlantic water of lower initial nutrient concentrations.

In this work we applied the three-components  $\delta^{18}\text{O}$ , salinity, and conservation of mass balance to derive the relative composition of the source waters in the Eurasian sector of the Arctic Ocean (Fig. 1). The model, together with preformed nitrate concentrations of the end members and a C/N ratio of 6.6, calculates the apparent carbon utilization, ACU. A relative degree of apparent carbon utilization, rACU with units %, is compiled and the computed rACU signal in the different layers along the shelf slopes and over the deep basins is used to evaluate the magnitude and fate of produced organic matter along the flow path. The findings reflect the importance of the shelf seas in sequestering carbon dioxide, and the shelf water plumes in transporting the subsequently nutrient impoverished waters to the intermediate and deep waters over the basins.

### Acknowledgments

<sup>1</sup> Present address: Akvaplan-niva AS, Tromsø, Norway.

The oceanographic groups and crew on board IB *Oden* and RV *Polarstern* are gratefully acknowledged for their assistance during the *Oden—91* and *ARK IX—4* expeditions. We are thankful to G. Mathieu for the collection and analysis of the CFC data during the *ARK IX—4* expedition, and to C. Facklam and R. Neubert who performed the <sup>18</sup>O analysis on the samples collected during the same expedition. K. Olsson and L. G. Anderson received financial support from the Swedish Natural Science Research Council and Swedish Environmental Protection Agency, and this work was a contribution within the Swedish Arctic Research program. M.F. and B.S. received financial support from the German Science Foundation and NSF grant OPP 93–03026, respectively. The authors also thank U. Schauer, D. Dyrssen, and R. Bayer for valuable comments and discussions on the manuscript.

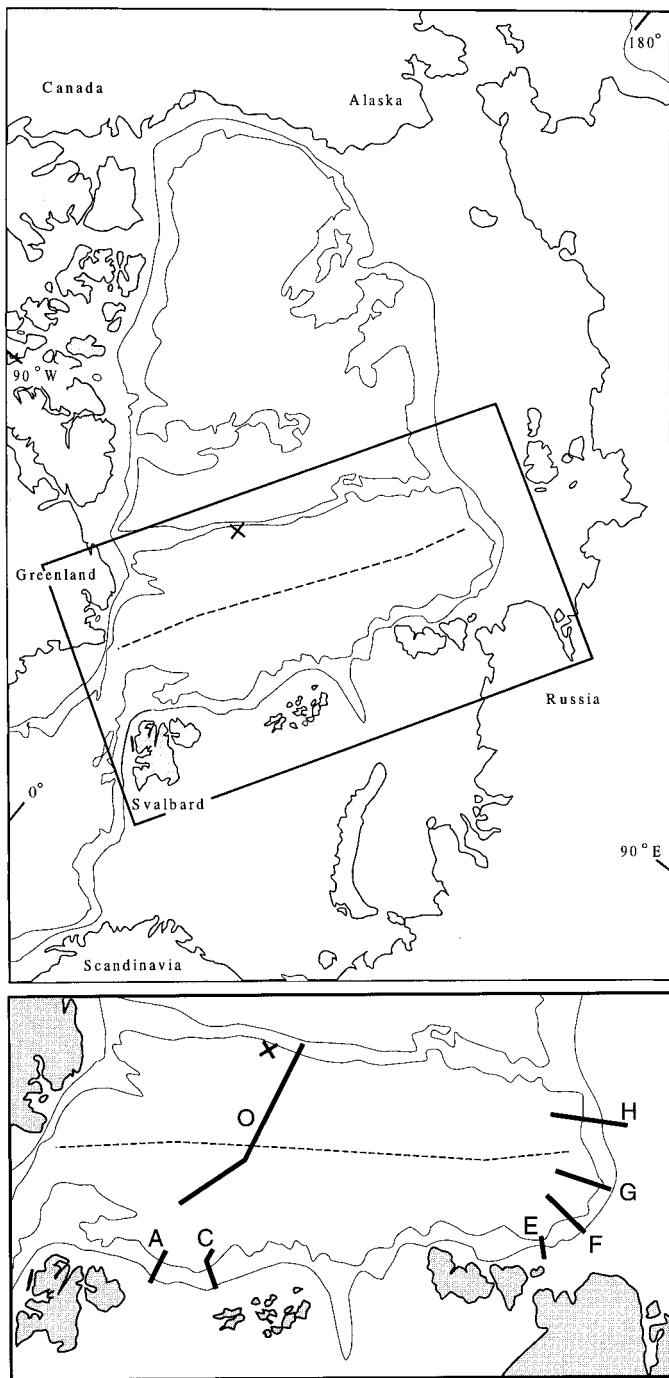


Fig. 1. The Arctic Ocean with an expansion of the investigated area. Sections A–C and E–H were covered in 1993 during the ARK IX–4 expedition by RV *Polarstern* while the deep section O was sampled during the *Oden–91* cruise.

## Methods

The data set used in the model is based on seawater samples collected during the *Oden–91* and *Polarstern–93* (ARK IX–4) expeditions. The German RV *Polarstern* operated along the shelf slopes of the Barents and Laptev Seas in 1993 (6 August to 5 October), while the Swedish IB *Oden*

in 1991 (1 August to 14 October) covered the deep Nansen, Amundsen, and parts of the Makarov Basin. Section locations for the ARK IX–4 and the section of the *Oden–91* expedition used in this contribution are shown in Fig. 1.

Salinities were determined during both expeditions with a Guildline Autosal 8400 B salinometer, and potential temperature was calculated from temperature data obtained from a Neil Brown Mark III conductivity-temperature-depth (CTD) system. Precision and accuracy for both parameters are given in Schauer et al. (1997) and in Anderson et al. (1994a) for the ARK IX–4 and *Oden–91* cruises, respectively. Nitrate was determined according to the method of Grasshoff (1983) with a precision of 1.2%.

Determination of the  $\text{H}_2^{18}\text{O}/\text{H}_2^{16}\text{O}$  ratio in seawater samples was carried out using a MAT 252 mass spectrometer, after equilibration of the water samples with  $\text{CO}_2(\text{g})$ , following procedures described by Roether (1970). The results are reported in  $\delta^{18}\text{O}$  (‰) notations as per mille deviation of the  $\text{H}_2^{18}\text{O}/\text{H}_2^{16}\text{O}$  ratio of the samples from that of standard mean ocean water (SMOW). Precision of the data is about 0.03‰.

Chlorofluorocarbons (CFCs) were measured on board using a purge and trap system interfaced to a Shimadzu 8A gas chromatograph equipped with an electron capture detector as described by Smethie et al. (1988) and Bullister and Weiss (1988). The samples were collected in 100-ml glass syringes from the 10-liter Niskin bottles attached to the rosette. The precision of the analysis was the greater of 0.8% or  $0.008 \text{ pmol kg}^{-1}$ .

## Results

**Source waters**—Three source waters dominate in the Eurasian sector of the Arctic Ocean, i.e., Atlantic water; sea ice-melt water, and river runoff. A model of mixing between these end members is created using salinity,  $\delta^{18}\text{O}$ , and conservation of mass, based on the equations presented by Östlund and Hut (1984), Schlosser et al. (1994), and Bauch et al. (1995). From this model, the fraction of each water mass represented in the water sample is calculated. For the mixing calculation, the salinity and  $\delta^{18}\text{O}$  of the Atlantic source water are set to 35 and 0.3‰, representing the least-modified Atlantic water that was found in the Arctic Ocean during the ARK IX–4 expedition (Fram Strait branch, section A).

The amount of salt enclosed in sea ice depends on the ambient conditions during the freezing process and on aging (e.g., Untersteiner 1986). Because sea ice forms seasonally over the shelves, the corresponding sea ice-melt contribution is assumed to be rather young. A salinity of 4.5 was therefore chosen on the basis of salinity intervals given by Untersteiner (1986). During sea ice formation,  $^{18}\text{O}$  enrichment occurs relative to the seawater from which it was formed. However, because the origin of the source water is difficult to deduce, we make a first-order approximation that the sea ice is formed from the surface water at the sampling location. Using the degree of fractionation determined by Mellling and Moore (1995) during sea ice growth over the Beaufort shelf, we set  $O_i = O_{\text{surface}} + 2.1\text{‰}$ .

Létolle et al. (1993) give  $\delta^{18}\text{O}$  values for Eurasian rivers west of the Yana, and from these values together with those

Table 1. Salinities,  $\delta^{18}\text{O}$  (‰), and preformed nitrate concentrations utilized in the model.

Source water	Salinity	$\delta^{18}\text{O}$ (‰)	Nitrate ( $\mu\text{mol kg}^{-1}$ )
Atlantic	35*	0.3*	12.5§
Sea ice-melt water	4.5†	( $O_{\text{surface}} \pm 2.1\%$ )†	1.6
River runoff	0‡	-21‡	3¶

\* Salinity and  $\delta^{18}\text{O}$  in the Fram Strait branch north of the Barents Sea during the *ARK IX-4* expedition (M. Frank unpubl. data).

†  $\delta^{18}\text{O}$  fractionation from Melling and Moore (1995); salinity from Untersteiner (1986).

‡  $\delta^{18}\text{O}$  from Létolle et al. (1993), Östlund and Hut (1984), and Bauch et al. (1995).

§ Mean winter concentration in the upper 500 m west of Bear Island derived from the Hudson cruise 82-001 (1984) and *ESOP-95* (T. Johannessen pers. comm.).

|| Deduced from the concentration in the Atlantic water and the assumed linear relationship with salinity and a sea ice salinity of 4.5.

¶ Mean of nitrate concentrations in Arctic rivers (Telang et al. 1991; Gordeev et al. 1996).

obtained by Östlund and Hut (1984) and Bauch et al. (1995), -21‰ was adopted, because the main fluvial contribution into the investigated area originates from the rivers Ob, Yenisei, and Lena.

*Fractionation of source waters*—The fraction of the source waters in each sample is calculated from  $\delta^{18}\text{O}$ , salinity, and conservation of mass according to

$$f_a + f_r + f_i = 1 \quad (1a)$$

$$f_a \times S_a + f_r \times S_r + f_i \times S_i = S_m \quad (1b)$$

$$f_a \times O_a + f_r \times O_r + f_i \times O_i = O_m \quad (1c)$$

where  $f_a$ ,  $f_r$ , and  $f_i$  are, respectively, the fractions of Atlantic water, river runoff, and sea ice-melt water, and  $S_a$ ,  $S_r$ ,  $S_i$ ,  $O_a$ ,  $O_r$ , and  $O_i$  are the corresponding salinities and  $\delta^{18}\text{O}$  values (Table 1).  $S_m$  and  $O_m$  are the measured salinity and  $\delta^{18}\text{O}$  values of the seawater samples. A positive  $f_i$  is regarded as melt water in the resulting model while negative values can be interpreted as addition of brine.

*Preformed concentrations*—The term preformed nitrate here represents the nitrate in the source waters entering the Arctic Ocean. The preformed nitrate concentration,  $[\text{NO}_3]_0^0$  with units  $\mu\text{mol kg}^{-1}$ , in the Atlantic water is deduced from the winter data collected in the upper 500 m west of Bear Island (74°N, 15°E) during the *ESOP-95* expedition (T. Johannessen pers. comm. 1997) and the *Hudson-82* cruise (Scripps Institution of Oceanography 1984), as this site represents the region where the Atlantic water diverges into the Fram Strait and the Barents Sea. By choosing winter data, the effect of potential production in the source water prior to entering the Arctic Ocean is reduced. Summer data from the same region has the similar mean concentration between 100 and 500 m, while the water in the upper 100 m show the expected deficit due to primary production.

Riverine nitrate concentrations are taken from Telang et al. (1991) and Gordeev et al. (1996) and are in the range of 2.0–3.2  $\mu\text{M}$  in the rivers entering the Kara and Laptev Seas.

Because the authors do not report seasonal variabilities in concentration or discharge, this concentration is somewhat uncertain. However, as can be seen from the calculations performed here, the computations are not that sensitive to the runoff nitrate concentration. For the sea ice-melt water, the underlying assumption is that no fractionation of nitrate takes place during the formation of sea ice (e.g., Assur 1958). From this argument follows a linear relationship between the preformed nitrate concentration and salinity, i.e.,

$$[\text{NO}_3]_i^0 = \frac{S_i[\text{NO}_3]_a^0}{S_a} \quad (2)$$

Nitrate was chosen as the input parameter because the production of marine phytoplankton is often nitrogen limited (e.g., Dugdale and Goering 1967; Ryther and Dunstan 1971; Jones et al. 1984). The most obvious drawback with this approach is denitrification, i.e., loss of combined nitrogen to nitrous gases in low dissolved oxygen environments (e.g., Codispoti 1989). The subsequent removal of nitrate would be incorporated in our calculations, resulting in an overestimate of the carbon utilization. However, Wilson and Wallace (1990) found NO/PO signal  $\sim 1$  throughout all water masses in the Eurasian Basin, which suggests denitrification in the Eurasian shelves to be of minor importance. The properties NO ( $=[\text{O}_2] + 9[\text{NO}_3]$ ) and PO ( $=[\text{O}_2] + 135[\text{PO}_4]$ ) are conservative as they account for the simultaneous changes in oxygen and nutrient concentrations during biological processes (Broecker 1974). The distribution of nitrate along the sections investigated are shown in Fig. 2.

The preformed concentration of each seawater sample,  $[\text{NO}_3]_m^0$ , is calculated from the relationship between seawater composition and preformed end-member concentrations according to

$$[\text{NO}_3]_m^0 = f_a[\text{NO}_3]_a^0 + f_r[\text{NO}_3]_r^0 + f_i[\text{NO}_3]_i^0 \quad (3)$$

This calculation is performed on all seawater samples collected during the *Polarstern-93* expedition, where  $\delta^{18}\text{O}$  were determined. For the *Oden-91* samples and the rest of the *Polarstern-93* samples, a simplified model was made where a linear relationship between salinity and preformed nitrate concentrations was achieved,

$$[\text{NO}_3]_m^0 = 0.30S_m + 1.97 \quad (4)$$

Where the intercept 1.97 is the mean of  $[\text{NO}_3]_r^0$  and  $[\text{NO}_3]_i^0$ . The simplification is justified by the fact that the relative amounts of these fresh waters are fairly small, and this results in an error less than  $\pm 0.6\%$ .

*Production and decay of organic matter*—When subtracting measured nitrate concentration from that of the preformed, a net estimate of the nitrate used for production or released during decay is obtained. This term is here denoted apparent nitrate utilization (ANU). By applying the Redfield stoichiometry between carbon and nitrogen (Redfield et al. 1963), the ANUs are converted to carbon equivalents, i.e., to ACU. Criticism regarding the Redfield-Ketchum-Richards (RKR) and other Redfieldian ratios has arisen (e.g., Shaffer 1996; Anderson and Sarmiento 1994), illuminating unresolved problems such as latitudinal (temperature) dependence on phytoplanktonic composition and vertical frac-

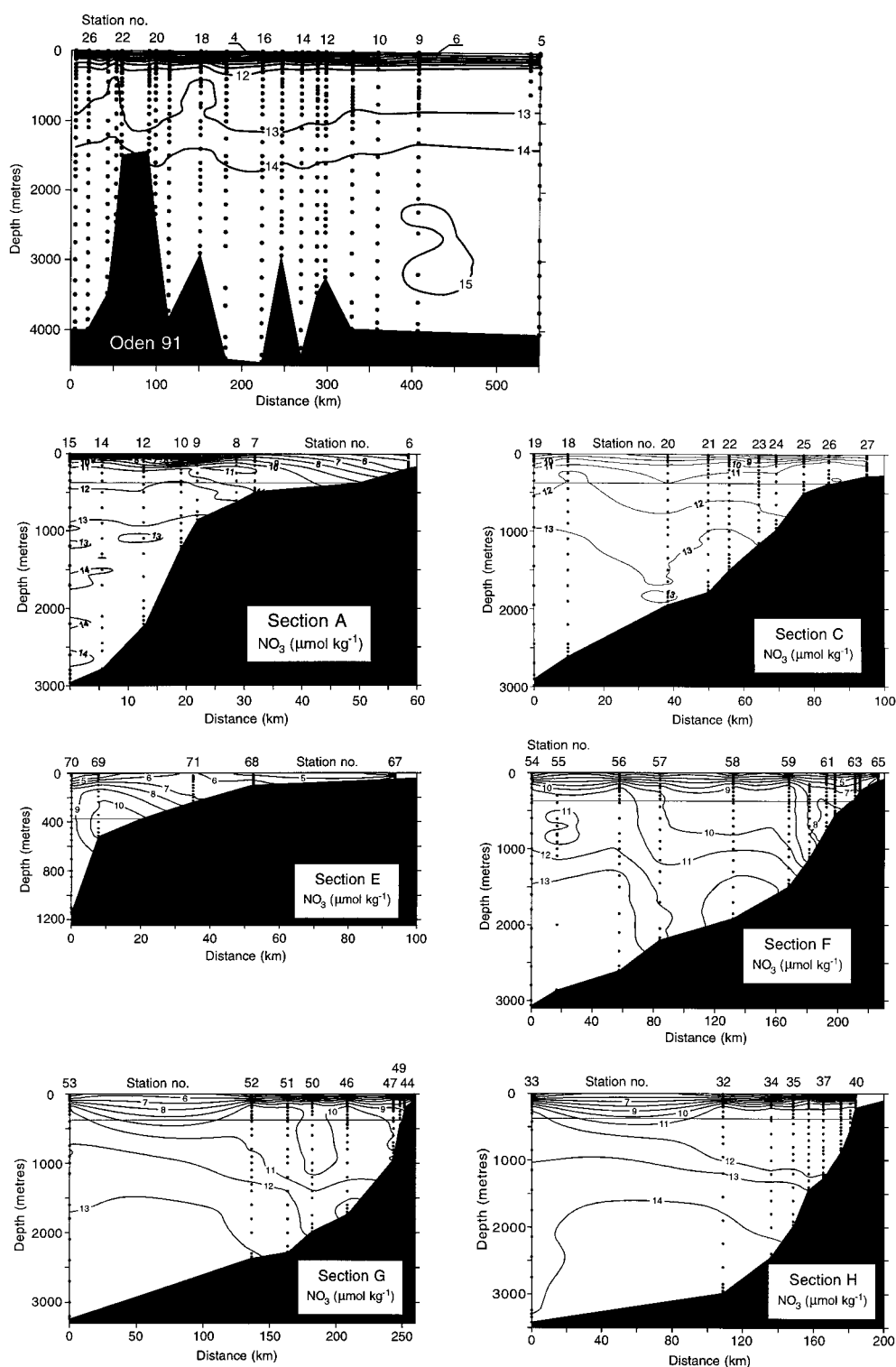


Fig. 2. The distribution of nitrate along the sections shown in Fig. 1.

tiation during settling of organic matter. While the RKR model illustrates the stoichiometric composition in phytoplankton, other observations (e.g., Takahashi et al. 1993; Anderson and Sarmiento 1994) relate the ratios between nutrients, carbon, and dissolved oxygen instead by looking at

decay of organic matter in the deep oceans. However, vertical preferential degradation is likely to occur during settling while the latter approach would not be representative of the nutrient consumption during production. Because we relate shelf-exported carbon to estimates of productivity we choose

to apply the RKR C/N ratio of 6.6. However, even in surface water the consumption of nitrogen to carbon might not follow the traditional RKR ratio as a result of different effects, including preferential remineralization of nitrogen in the photic zone, resulting in an underestimate of the carbon export of up to 20% (Sambrotto et al. 1993).

A relative degree of ANU, rANU with units in % can be obtained by dividing the ANU with the preformed nitrate concentration of the sample. The distribution of the rACU equals that of rANU and is shown in Fig. 3.

*Definition of layers*—The definitions of layers 1–4 are based on a combination of the classical water mass definitions and the outcome of the model with respect to rACU values. Layer 1 extends from the surface down to the depth of salinity 34.3 and hence equals the sum of the conventional surface mixed layer and the lower halocline. The lower boundary of the layer 2 corresponds to 375 m for reasons given below and resembles the traditional Atlantic layer. A third boundary is set where the rACU concentrations equal zero, so the layer 4 is represented by negative values of rACU and extends to the bottom.

The seasonal transformation of surface water along the investigated area (Rudels et al. 1996) makes it appropriate to combine the surface mixed-layer and lower halocline waters into the top layer. The lower boundary of layer 2 originates from the depth in the deep basin where rACU approximately equals zero. The same corresponding depth is chosen, 375 m, for all sections, even if the density varies slightly. The classical definition of the Atlantic layer, i.e., temperature greater than 0°C, first suggested by Nansen (1902), is not suitable along the Laptev Sea slope because the Barents Sea branch of Atlantic water is colder than the Fram Strait branch at the same depth.

*General circulation*—The ACU distribution along the Barents and Laptev slopes is consistent with the general circulation scheme of intermediate waters, i.e., with a boundary current flowing eastward along the continental slopes (e.g., Rudels et al. 1994). In addition to the branch of Atlantic water entering the Arctic Ocean north of Svalbard, Atlantic water that has been modified while traversing the Barents Sea enters at the St. Annas Trough and displaces the Fram Strait branch toward the interior (Schauer et al. 1997). Part of this subsurface current will deflect and follow the ridge topography poleward north of the Laptev Sea (Rudels et al. 1994), while the remaining current continues east into the Canadian Basin. At the Laptev Sea shelf break, low salinity water of high runoff content enters the surface water over the deep interior and follows the Siberian branch of the Transpolar Drift toward the Fram Strait (Anderson et al. 1994b). The deep and bottom waters within the Eurasian sector largely follow a cyclonic circulation scheme, with additional recirculation in the Nansen and Amundsen Basins, including some entrainment of water from the Canadian Basin (Anderson et al. 1994a).

*Residence times and volume flows*—For layer 2, the average CFC-11 and CFC-12 concentrations along section C are 5.2 and 2.5 pmol kg<sup>-1</sup>, respectively, corresponding to an

age of 5–7 yr if the water was formed at 100% saturation. With a flow speed of 5 cm s<sup>-1</sup> as suggested by Aagaard (1989), the corresponding time period would be 40 d. Obviously, the resulting CFC-11 age is much too high, which can be ascribed to the degree of saturation being less than 100% when the water left the surface. In order to minimize the problem associated with uncertainty in the degree of saturation, we use the percent difference in CFC concentrations of the Fram Strait branch between sections C and F to estimate the transit time between these locations. The percent differences equal 4.1 and 8.8% in CFC-11 and CFC-12, respectively, and reflect recent atmospheric trends resulting from the Montreal Protocol. Subtracting a time lag from when the water was last in contact with the atmosphere of 1–2 yr (Wallace et al. 1992) and comparing the observed values with the annual percent change in the Northern Hemisphere for the last few years based on recent atmospheric measurements (Elkins et al. 1993; Cunnold et al. 1994) yields a transport time of 3 ± 1 yr. This transport time will be applied for the Fram Strait branch in the two uppermost layers, assuming these layers to flow with the same speed.

Rudels (1987) calculated the flow of Atlantic water through Fram Strait from two CTD sections across the strait, assuming geostrophic balance. He concluded that a flux of 1.9 Sv of Atlantic water passed the section of which half recirculated into the northern part of the strait, while the remaining half continued into the Arctic Ocean. The inflow from the Nordic Sea across the Barents Sea of 1.2 Sv was calculated by Rudels (1987) from a heat balance, while Pfirman et al. (1994) concluded 2 Sv based on current measurements from Loeng et al. (1993), data that also show the large variability of this inflow. Based on these estimates, we have chosen a total inflow rate for the Atlantic water of 1 Sv through Fram Strait and 1.5 Sv across the Barents Sea.

These flows are then subdivided into the different layers, where 0.2 Sv from the Atlantic inflow originating from the Fram Strait (Steel et al. 1995; Anderson et al. 1997) enters layer 1 and the remaining (0.8 Sv) of the same current flows into layer 2 (Anderson et al. 1997). The Barents Sea branch is subdivided into four outflow paths, i.e., 0.2 Sv enters layer 1 (Steel et al. 1995; Anderson et al. 1997), 0.15 Sv (Anderson et al. 1997) flows into the Laptev Sea through Vilkitsky Strait, while the rest flows into layers 2 and 3. According to Bönisch and Schlosser (1995), the volume flowing to layer 3 equals 0.30 Sv, while the residual of the 1.5 Sv of the Barents Sea branch inflow, i.e., 0.85 Sv, must enter layer 2. Water from the Norwegian Sea flows into layer 4, which according to Bönisch and Schlosser (1995) amounts to 0.58 Sv. Part of the Barents Sea inflow of 0.3 Sv to layer 3, i.e., about 0.04 Sv, will, according to the same authors, mix into the deep layers of the Eurasian Basin and thereby contribute to the inflow to layer 4.

*Distribution of rACU*—We distinguish between the two branches of Atlantic water, i.e., the Fram Strait and Barents Sea branches, on the basis of salinity, potential temperature and transient tracer data along with the different rACU concentrations. The following discussion includes processes occurring over the shelves adjacent to the slope sections investigated.

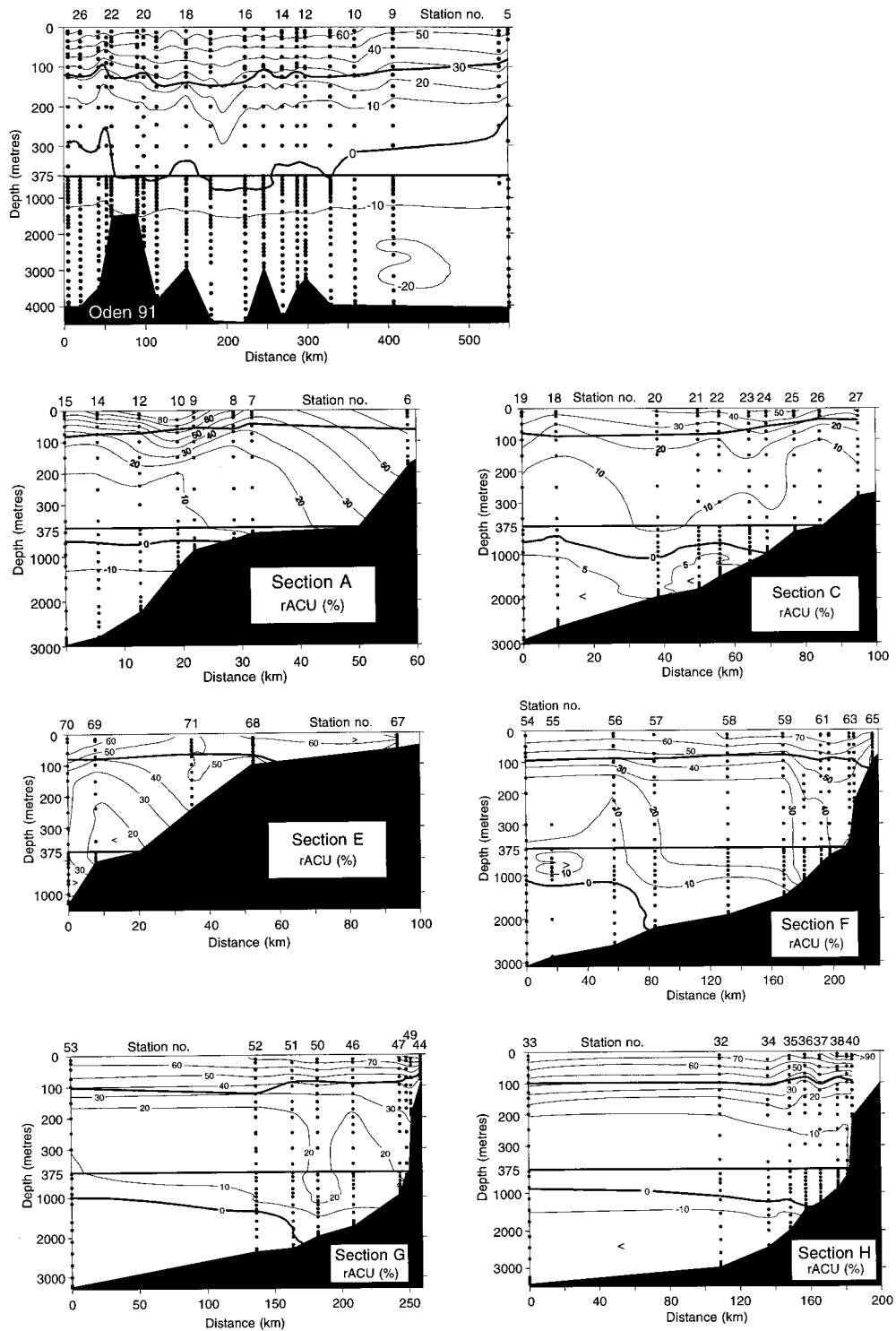


Fig. 3. The distribution of rACU along the sections shown in Fig. 1. For each section, division into four water layers has been made according to: layer 1 represents the seasonally transformed upper water column (upper 75–100 m), separated from layer 2 by the salinity of the lower halocline, 34.3. The second layer (layer 2) extends to 375 m, a depth derived from the depth of zero ACU over the deep basin. Layers 3 and 4 are divided by the depth of zero ACU over the shelf slopes.

*Layer 1: Salinity < 34.3*—A relative degree of apparent carbon utilization of 35–80% are found in section A (Fig. 3). These figures are higher than in section C where the values are 20–40%. When reaching the Laptev Sea slope (sections F–H), the rACU increases to about 40–70%. Although some patchiness is evident, the latter numbers are rather homogeneous. In the Nansen Basin (*Oden*—91 Stas. 5–10), the rACU values (30–50%) are slightly higher than those in section C. From the Nansen–Gakkel Ridge (*Oden*—91 Stas. 12–15), across the Amundsen Basin and the Lomonosov Ridge (*Oden*—91 Stas. 20–24), the rACU values are constant in the range 30–60%.

The mean value of 55% found in section A equals a net production of  $42 \text{ g C m}^{-2}$ , using an average layer thickness of 75 m. With the mean in section C of 34%, the corresponding production is  $26 \text{ g C m}^{-2}$ . Compared with section C, the ACU values of section A are higher and patchy, reflecting recent primary productivity within the latter section. Section A lies close to the ice edge, while C was ice covered during the time of investigation, which supports the idea of high rACUs in A being attributed to local production. Because A is under a strong influence of biological activity, we have chosen section C as representative of inflowing water entering layer 1 through the Fram Strait. The local production at section A hence corresponds to the difference in productivity between sections A and C, i.e.,  $16 \text{ g C m}^{-2}$ , which is very close to estimates in other marginal ice zone regions (e.g., Yager et al. 1995) influenced mainly by Atlantic water.

When reaching the Laptev Sea margin, the rACUs have increased to ~61% (mean of Stas. 32–33 and 52–57). The difference in ACU content of 27% (61–34%) between the slope sections C and the outermost stations of F–H corresponds to an in situ production of  $0.5 \pm 0.2 \times 10^{12} \text{ g C yr}^{-1}$  along the Kara shelf slope, when applying the volume inflow ( $0.2 \text{ Sv}$ ) and residence time ( $3 \pm 1 \text{ yr}$ ) of the Fram Strait branch as stated above.

To deduce the rACU values in the waters flowing off the Barents–Kara and Laptev slope, respectively, we study the salinity and rACU depth profiles of sections F and G (Fig. 4). In both profiles a sharp bend in rACU is seen at 35 m (Fig. 4A) and 50 m (Fig. 4B) depth, which coincide with the lower boundary of a sharp salinity gradient. These depth levels are taken as the boundary between the waters of the Laptev and Barents–Kara shelf outflows, respectively, where the Laptev shelf water has the lower salinity. The Barents–Kara shelf water constitutes the layer between this boundary and the level of salinity 34.3, that of the lower halocline. The average rACU values obtained are 78 and 55% (Fig. 4A, 4B) as originating from the Laptev and Barents–Kara Seas, respectively.

Combining the rACUs with the volume inflows, i.e.,  $0.16 \text{ Sv}$  from the Laptev Sea and  $0.2 \text{ Sv}$  from the Barents–Kara Seas (Steel et al. 1995; Anderson et al. 1997), results in shelf exports of  $4.0$  and  $3.5 \times 10^{12} \text{ g C yr}^{-1}$ , respectively. The underlying assumption for this type of calculation is that we can apply to the Barents Sea branch inflows into all layers the same  $[\text{NO}]_0^0$  as that within the Fram Strait branch north of the Barents Sea. However, production might take place in the surface water prior to entering our investigation area.

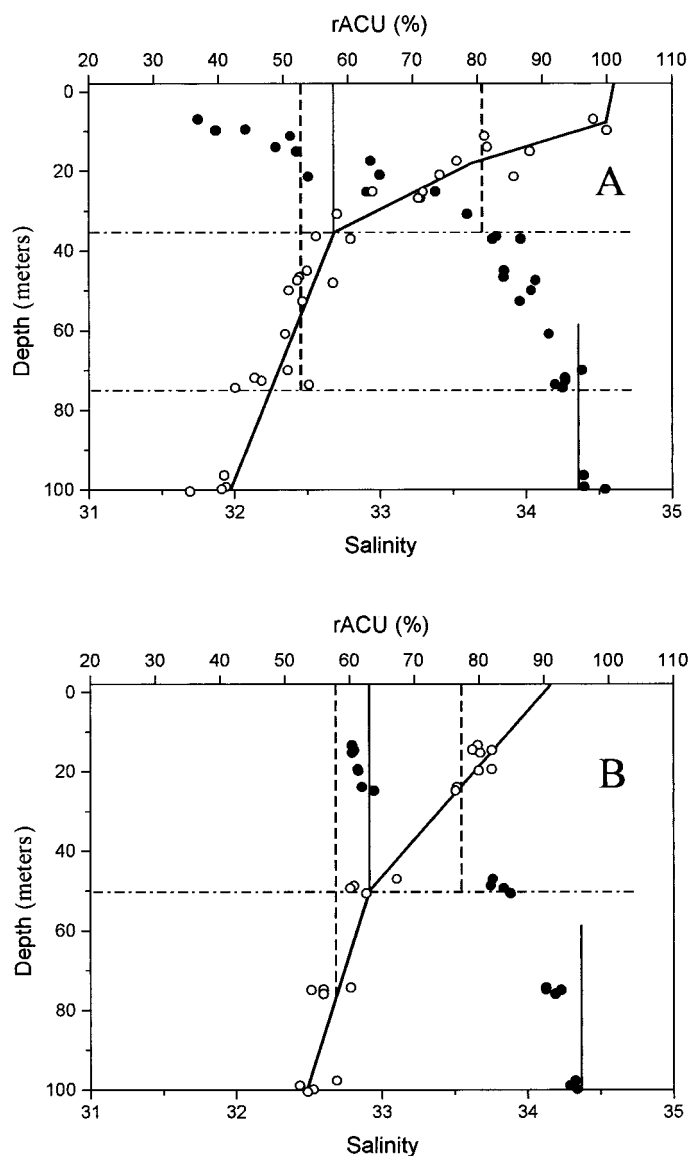


Fig. 4. The average depth profiles of salinity (filled squares) and rACU (open circles) at the stations 44–49, section G (A) and stations 61–64, section F (B).

While we cannot discern such a potential productivity, we have at present to accept this assumption.

Most of the water in layer 1 north of the Laptev Sea is incorporated into the Siberian branch of the Transpolar Drift (e.g., Schlosser et al. 1994) flowing back toward Fram Strait over the Amundsen Basin. The outermost stations of sections F and G have similar rACU as those over the Amundsen Basin in section O (Fig. 3). This implies a low new production rate along this flow path. These findings suggest that the reported high productivity in and under the sea ice realm (e.g., Wheeler et al. 1996) is dominated by recycled matter. Even if our results are confined to the Eurasian sector, it is difficult to imagine significantly different preconditions in other ice-covered regions.

*Layer 2: Salinity > 34.3, depth < 375 m*—In the Nansen Basin, the rACUs amount to 0–30% (*Oden*—91, Stas. 5–10)

with the values in sections A–C being 10–20% (Fig. 3). The stations closest to the shelf, especially in section A, have some anomalous values that are likely to have been caused by shelf-water intrusion (Schauer et al. 1997). The rACU values in sections F–H (10–40%) are higher than those in A–C, and they increase further toward the shelf. In addition to the observed lowering in rACU toward the interior of the basins, rACU also decreases eastward from section F to H by about 30% (45–15%) along the shelf break at depths less than 1,000 m. Section O reveals remarkably stable rACUs of about 10% both over the Amundsen Basin and across the two ridges.

The rACU values are two to four times lower in layer 2 than in layer 1. Although lower, they are still positive, i.e., a larger productivity than decay signal prevails. No in situ production is likely to occur within this layer as depths are well below the photic zone, while the rACU values are likely a result of advection. Furthermore, the rACUs are uniformly distributed in sections A–C, so no seasonal signal is expected to have a major influence on the interpretation.

The marked difference between the rACU values of the inner and outermost stations along the Laptev Sea (especially section F) reveals the existence of the two Atlantic branches, through their inherited difference in biological history. In section A–C the mean rACU within the Fram Strait branch is 15%, which is only slightly less than that found at the outer stations in sections F and G (mean for Stas. 53–56 equals 16%). This difference is within the variability so our data do not indicate any decay of organic matter within this Fram Strait branch, while flowing along the continental slope at the southern Nansen Basin.

Between the outermost stations of F and G and section O, rACU decreased from 16 to 10% (mean for *Oden*—91 Stas. 11–21). This difference implies an en route mineralization of at least  $17 \text{ g C m}^{-2}$ , as the mean depth of this layer is about 275 m. Wallace et al. (1992) estimated a tracer age of 10–15 yr for the Atlantic layer over the Nansen–Gakkel Ridge at the O section. According to the same authors, about one third of this age could be attributed to the transit from Fram Strait to the Laptev Sea, which results in a transport time of 7–10 yr between sections F and G and O. This in turn implies a decay rate of  $1.7$ – $2.4 \text{ g C m}^{-2} \text{ yr}^{-1}$ . However, not all Atlantic layer water along the Eurasian shelf slope flows back to the Fram Strait within the Eurasian sector but instead enters the Canadian Basin prior to exiting through the Fram Strait. If half of the inflowing water to layer 2, i.e.,  $\sim 0.9 \text{ Sv}$ , is taken to recirculate within the Eurasian sector, this would correspond to a flux of about  $-0.2 \times 10^{12} \text{ g C yr}^{-1}$ .

In sections F and G, the high rACU shallower than the 1,000-m isobath (Stas. 57–61 and 47–50) has a shelf source dominated by the Barents–Kara Seas (Schauer et al. 1997). With the same arguments as for layer 1 we use the mean rACU value from the stations with highest shelf contribution in section F, which for layer 2 equals an rACU of  $\sim 43\%$  and the inflow of  $0.85 \text{ Sv}$  from the shelf plume to calculate the shelf export. The obtained estimate of  $12 \times 10^{12} \text{ g C yr}^{-1}$  is about twice that exported to layer 1, which can be attributed to the larger inflow to the deeper layer of the two. In turn, the eastward decrease in rACU along the Laptev

slope is attributed to extended mixing with water from the deeper stations.

*Layer 3: Depths > 375 m, ACU > 0*—The stations in section O all have rACU very close to zero at depth around 375 m (Fig. 3), in accordance with our selection of layers definitions. A general trend in this layer is the lower rACU along the Barents slope than in the Laptev Sea. In sections A–C the rACU is below 5% except for stas. 7 and 8 that have somewhat higher rACU (11%). In the Laptev Sea, the rACU increases southward, from 4 to 9% up to 35%, reflecting the outflow of water from the Barents–Kara Seas.

Inflowing Fram Strait branch water contributes to the positive rACUs along sections A–C because Atlantic layer water with temperature greater than  $0^\circ\text{C}$  penetrates deeper than 375 m along the slope. The elevated rACUs at Stas. 7 and 8 on the other hand reflect a signal from the Barents Sea shelf water intrusion (Schauer et al. 1997), which was also seen in layer 2. The outermost stations in sections F–H show similar rACU values as in sections A–C, which is in agreement with the transient tracer data, while both properties increase toward the shelves in the former sections. The simultaneous increases in rACU and CFC (data not shown) concentrations are clear indications of intrusion of a more recently ventilated shelf water, carrying a production signal. As in layer 2, the eastward decrease along F–H is attributed to increased mixing with water from deeper stations that are low in rACU. For this reason it seems appropriate to choose the rACUs at the shelf break stations at section F as representatives of the pure Barents Sea branch water. The average rACU of 33% for these stations together with an inflow of  $0.26 \text{ Sv}$  (Bönisch and Schlosser 1995) from the Barents and Kara Seas results in an estimated shelf export to this layer of  $2.8 \times 10^{12} \text{ g C yr}^{-1}$ .

*Layer 4: ACU < 0*—In sections A–C, the mean rACU equals  $-6\%$  while sections F and G are higher by 2%, as a result of penetration of high rACU shelf water (Fig. 3). This is consistent with the observation of layer 3 extending down to more than 2,000 m along the Laptev slope while it extends to less than 1,000 m close to the continental shelf break along the Barents slope. The average rACU along section O is  $-13 \pm 2\%$ . Mean rACUs of section H fall in between those of sections O and F and G.

Negative rACUs reflect the effect of in situ mineralization and/or advection of nutrient-enriched waters. Because the rACUs within this layer are lower in the central basin than along the slopes, the latter regimes must have been supplied with water of more recent shelf origin. As in layers 2–3, this shelf water intrusion signal decreases eastward along the Laptev slope, indicating progressive mixing with water from the deeper stations. The lower rACUs at sections A–C relative to F and G are attributed to inflow from the Norwegian Sea through the Fram Strait. Comparison with nutrient data collected in the Norwegian Sea during the *ESOP*—95 cruise (T. Johannessen pers. comm.) yields a mean rACU of  $-4\%$ , which strengthens the argument given above.

Assuming steady state, the relative input of rACU should equal the sum of rACU found over the deep basins ( $-13 \pm 2\%$ ) and that decayed in the interior. The Norwegian Sea

inflow contributes with 0.58 Sv (Bönisch and Schlosser 1995) and a mean rACU of  $-4\%$  (T. Johannessen pers. comm.), i.e.,  $-0.75 \times 10^{12} \text{ g C yr}^{-1}$ , to which the shelf contribution from layer 3 ( $2.8 \times 10^{12} \text{ g C yr}^{-1}$ ) should be added along with the small shelf intrusion of 0.04 Sv to layer 4. Although deduced, the latter inflow has never been observed so no corresponding rACU can be given. To avoid overestimating the shelf export, the rACU in this shelf water intrusion is set to zero, while the volume flow has to be added to the total inflow to this layer. Taken together, these three inflows equal  $2.0 \times 10^{12} \text{ g C yr}^{-1}$  from which the outflow,  $-3.7 \times 10^{12} \text{ g C yr}^{-1}$  (0.88 Sv,  $-13\%$ ) from layer 4 should be subtracted, yielding a remineralization rate of  $5.7 \times 10^{12} \text{ g C yr}^{-1}$  within the deep basins. This estimate includes any possible negative rACUs flowing off the shelf break, within the 0.04 Sv.

**Barents–Kara Sea production**—Adding up the ACU fluxes from the shelf seas to layers 1–3, we obtain an annual carbon export from these seas of  $22.3 \times 10^{12} \text{ g C yr}^{-1}$ . Subtracting the contribution from the Laptev Sea ( $4 \times 10^{12} \text{ g C yr}^{-1}$ ), the remaining  $18.4 \times 10^{12} \text{ g C yr}^{-1}$  can be attributed to the Barents Sea. The distance from the Norwegian Sea to the St. Annas Trough is about  $1.5 \times 10^6 \text{ m}$ , which, combined with a current width of  $0.2 \times 10^6 \text{ m}$  (Rudels 1987), results in a new production of  $\sim 60 \text{ g C m}^{-2} \text{ yr}^{-1}$ . Considering the uncertainties in production area and residence time, this is in agreement with model estimates of  $40\text{--}90 \text{ g C m}^{-2} \text{ yr}^{-1}$  (Slagstad and Wassman 1996) even if this estimate includes total production.

**Uncertainties and sensitivity of the model**—Essentially five sources contribute to the uncertainty of the overall results, for which variabilities in volume flows and the estimates of residence times dominate. Because the obtained rACUs are divided or multiplied by residence times and volume flows, of which both are uncertain by up to 50%, the export yields will also vary within this range. In a system where volume flows and residence times are well known, the choice of Redfieldian ratio, preformed concentrations, and the sensitivity of the model with regard to input parameters will contribute to the uncertainties of the estimated shelf export. As mentioned above, the carbon export could exceed the total production as estimated based on nitrogen consumption by up to 20% (Sambrotto et al. 1993). Furthermore, potential degradation below 400 m has been observed with a subsequent increase in C/N ratio of up to 10% (Anderson and Sarmiento 1994). Hence, the rACU levels, and thereby the degree of mineralization, of layer 4 could be underestimated by the same factor.

A  $1 \mu\text{mol kg}^{-1}$  deviation in the preformed nitrate concentration of the Atlantic water would equal a 4% deviation in rACU. Hence, an export production of  $12 \times 10^{12} \text{ g C yr}^{-1}$  would differ by  $0.5 \times 10^{12} \text{ g C yr}^{-1}$ , which is on the order of the Fram Strait branch production to the upper layer. However, while deviation from the true end-member concentrations will affect the absolute figures, the relative distribution pattern would not be expected to become affected.

The sensitivity of the model was tested by independently varying the input parameters within reasonable limits. The

Flux in $10^{12} \text{ g C yr}^{-1}$			Laptev Sea
Eurasian Basin	Fram Strait Branch	Barents Sea Branch	$4.0 \pm 2.0$
0	$0.5 \pm 0.2$	$3.5 \pm 1.7$	Layer 1
$-0.17 \pm 0.05$	0	$12 \pm 6$	Layer 2
	0	$2.8 \pm 1.4$	Layer 3
$-5.7 \pm 2.3$	$-0.8 \pm 0.4$	N.D.	Layer 4
<b><math>-5.9 \pm 2.3</math></b>	<b><math>-0.3 \pm 0.5</math></b>	<b><math>22.3 \pm 6.7</math></b>	<b>Total</b>

Fig. 5. Summary of the fluxes of carbon utilized (Gton C yr<sup>-1</sup>) to the Eurasian Basin for each layer, branch, and the basin section (○) in the Eurasian section of the Arctic Ocean. ND indicates that no dense shelf water plume signal could be detected (nondetectable). The errors noted correspond to estimated uncertainties in volume flows and residence times.

test was performed for all layers on stations with river-runoff content extremes. No output combination resulted in an error larger than  $\pm 0.5\%$  of the preformed values. All of these uncertainties are within the precision of the nitrate determinations (1.2% SD) and are far less than the other uncertainties given above.

## Conclusions

Figure 5 summarizes the overall inventory of exported ACU for each layer and branch within the Eurasian sector of the Arctic Ocean. From these estimates, the following conclusions can be drawn.

The shelf seas totally dominate productivity in this region, as shown by the export production of  $0.022 \pm 0.007 \text{ Gton C yr}^{-1}$ . Shelf export for the Arctic Ocean is  $0.053 \text{ Gton C yr}^{-1}$ , which was estimated by combining our findings with that of the Canadian shelf sector (Anderson et al. 1994b). Thus the total shelf export production to the Arctic Ocean equals around  $0.07 \text{ Gton C yr}^{-1}$ , corresponding to a mean of  $15 \text{ g C m}^{-2} \text{ yr}^{-1}$  when the area of all the Arctic shelves ( $4.5 \times 10^{12} \text{ m}^2$ ) is considered. Although the total shelf export is small on a global scale the polar regions are one of the areas thought to be most affected by climatic changes because the sequestering of carbon dioxide potentially is significantly altered (Walsh et al. 1989; Codispoti et al. 1991).

Shelf water intrudes into all water masses (layers), which is clearly seen from the rACU distribution (Fig. 3). Because positive rACU values can be obtained only in a water where primary production occurs, the origin of this signal must come from the shelves as no contribution from the Fram Strait branch was observed. If shelf water intrusion had not

occurred, the depth of zero rACU would equal that of the lower boundary of the Atlantic layer (~375 m). Instead, we observed the zero rACU depth to increase southward, indicating the intrusion depths. This transport mechanism, i.e., of surface water deposited into deeper layers, is the criterion for long-term sequestering of carbon dioxide (Sarmiento and Toggweiler 1984).

The remineralization rate signal of  $5.7 \times 10^{12}$  g C yr<sup>-1</sup> in the deep Eurasian Basin relative to an apparent carbon utilization over the shelf of  $22.3 \times 10^{12}$  g C yr<sup>-1</sup> indicates that about 25% of the particulate nitrogen exported out of the shelf seas is remineralized. This remineralization can either take place at the shelf sediment surface, with subsequent export of the decay products, or in the deep Eurasian Basin, following an export of biological matter.

The differences in rACU within layer 1 between the outermost stations along the Laptev Sea slope and section O in the Amundsen Basin are only within the uncertainty of these values. It can thus be concluded that essentially all new production is concentrated over the shelves and shelf slopes. This finding strengthens the general consensus that production in and under the perennial ice cover is of minor importance for the overall new production estimates.

The ACU distribution follows the circulation scheme, i.e., an eastward moving boundary current along the continental slopes of the Eurasian sector, with northward deflecting branches along the ridges (Rudels et al. 1996). Our model calculation shows a deep intrusion of the Barents Sea branch along the Laptev Sea slope, with depths down to 2,200 in the Laptev Sea slope compared to about 1,000 in the Barents Sea slope sections.

## References

- AAGAARD, K. 1989. A synthesis of the Arctic Ocean circulation. *Rapp. P.-V. Reun. Cons. Int. Explor. Mer* **188**: 11–22.
- ALEXANDER V., H. J. NIEBAUER. 1981. Oceanography of the eastern Bering Sea ice-edge in spring. *Limnol. Oceanogr.* **26**: 1111–1125.
- ANDERSON, L. A., AND J. L. SARMIENTO. 1994. Redfield ratios of remineralisation determined by nutrient data analysis. *Global Biogeochem. Cycles* **8**: 65–80.
- ANDERSON, L. G., AND OTHERS. 1994a. Water masses and circulation in the Eurasian Basin: Results from the Oden—91 expedition. *J. Geophys. Res.* **99**: 3273–3283.
- , K. OLSSON, AND M. CHERICI. 1997. A carbon budget for the Arctic Ocean. *Global Biogeochem. Cycles* **12**: 455–465.
- , ——— AND A. SKOOG. 1994b. Distribution of dissolved inorganic and organic carbon in the Eurasian Basin of the Arctic Ocean, p. 255–262. *In* O. M. Johannessen, R. D. Muench, and J. E. Overland [eds.], *The polar oceans and their role in shaping the global environment*. Am. Geophys. Union.
- ASSUR, A. 1958. Composition of sea ice and its tensile strength. *Nat. Resour. Council Publ.* **598**: 106–138.
- BAUCH, D., P. SCHLOSSER, AND R. FAIRBANKS. 1995. Freshwater balance and the sources of deep and bottom waters in the Arctic Ocean inferred from the distribution of H<sub>2</sub><sup>18</sup>O. *Prog. Oceanogr.* **35**: 53–80.
- BÖNISCH, G., AND P. SCHLOSSER. 1995. Deep water formation and exchange rates in the Greenland/Norwegian Seas and the Eurasian Basin of the Arctic Ocean derived from tracer balances. *Prog. Oceanogr.* **35**: 12–52.
- BROECKER, W. S. 1974. “NO”, a conservative-mass tracer. *Earth Planet. Sci. Lett.* **23**: 441–448.
- BULLISTER, J. L., AND R. F. WEISS. 1988. Determination of CCl<sub>3</sub>F and CCl<sub>2</sub>F<sub>2</sub> in sea water and air. *Deep-Sea Res.* **35**: 839–853.
- CODISPOTI, L. A. 1989. Phosphorous vs nitrogen limitation of new and export production, p. 377–394. *In* W. H. Berger, V. S. Smetacek, and G. Wefer [eds.], *Productivity of the oceans: Present and past*. Wiley.
- , G. E. FRIEDRICH, C. M. SAKAMO, AND L. I. GORDON. 1991. Nutrient cycling and primary production in the marine systems of the Arctic and Antarctica. *J. Mar. Syst.* **2**: 359–384.
- CUNNOLD, D. M., AND OTHERS. 1994. Global trends and annual releases of CCl<sub>3</sub>F and CCl<sub>2</sub>F<sub>2</sub> estimated from ALE/GAGE and other measurements from July 1978 to June 1991. *J. Geophys. Res.* **99**: 1107–1126.
- DUGDALE, R. C., AND J. J. GOERING. 1967. Uptake of new and regenerated forms of nitrogen in primary productivity. *Limnol. Oceanogr.* **23**: 196–206.
- DUNBAR, M. J. 1981. Physical causes and biological significance of polynyas and other open water in sea ice, and others. p. 29–44. *In* I. Stirling and H. Cleator [eds.], *Canadian Wildlife Service*.
- ELKINS, J. W., AND OTHERS. 1993. Decrease in growth rate of atmospheric chlorofluorocarbons 11 and 12. *Nature* **64**: 780–783.
- GORDEEV, V. V., J. M. MARTIN, I. S. SIDOROV, AND M. V. SIDOROVA. 1996. A reassessment of the Eurasian River input of water, sediment, major elements, and nutrients to the Arctic Ocean. *J. Am. Sci.* **296**: 664–691.
- GRASSHOFF, K. 1983. Determination of nitrate, p. 143–150. *In* K. Grasshoff, M. Ehrhardt, and K. Kremling [eds.], *Methods of seawater analysis*, 2nd ed. Verlag Chemie.
- HORNER, R. 1990. Ice-associated ecosystems, p. 9–14. *In* L. K. Medlin and J. Priddle [eds.], *Polar marine diatoms*. British Antarctic Survey.
- JONES, E. P., D. DYRSSEN, AND A. R. COOTE. 1984. Nutrient regeneration in deep Baffin Bay with consequences for measurements of the conservative tracer NO and fossil fuel CO<sub>2</sub> in the oceans. *Can. J. Fish. Aquat. Sci.* **41**: 30–35.
- LÉTOLLE, R., J. M. MARTIN, A. J. THOMAS, V. V. GORDEEV, S. GUSAROVA, AND I. S. SIDOROV. 1993. <sup>18</sup>O abundance and dissolved silica in the Lena delta and Laptev Sea (Russia). *Mar. Chem.* **43**: 47–64.
- LOENG, H., V. OZHIGIN, B. ADLANDSVIK, AND H. SAGEN. 1993. Current measurements in the northeastern Barents Sea. ICES Statutory Meeting, C.M. 1993/C:41.
- MELLING, H., AND R. M. MOORE. 1995. Modification of halocline surface water during freezing on the Beaufort Sea Shelf: Evidence from oxygen isotopic ratios and dissolved nutrients. *Cont. Shelf Res.* **15**: 83–113.
- NANSEN, F. 1902. Oceanography of the North Polar Basin. *Norw. Polar Exped. 1893–96, Sci. Res.* **3**: 427.
- ÖSTLUND, H. G., AND G. HUT. 1984. Arctic Ocean water mass balance from isotope data. *J. Geophys. Res.* **89**: 6373–6381.
- PFIRMAN, S. L., D. BAUCH, AND T. GAMMELSRØD. 1994. The Northern Barents Sea: Water mass distribution and modification, p. 77–94. *In* O. M. Johannessen, R. D. Muench, and J. E. Overland [eds.], *The polar oceans and their role in shaping the global environment*. Am. Geophys. Union.
- PLATT, T., AND V. SUBBA RAO. 1975. Primary production of marine microphytes, p. 249–280. *In* J. P. Cooper [ed.], *Photosynthesis and productivity of different environments*. Cambridge Univ. Press.
- REDFIELD, A. C., B. H. KETCHUM, AND F. A. RICHARDS. 1963. The influence of organisms on the composition of sea water, p. 26–77. *In* M. N. Hill [ed.], *The sea*, v. 2. Wiley.

- REY, F., AND H. LOENG. 1985. The influence of ice and hydrographic conditions on the development of phytoplankton in the Barents Sea, p. 49–63. *In* J. S. Gray and M. E. Christiansen [eds.], *Marine biology of polar regions and effects of stress on marine organisms*. Wiley.
- ROETHER, W. 1970. CO<sub>2</sub> exchange set-up for routine 18 oxygen assay of natural waters. *Int. J. Appl. Radiat. and Isot.* **21**: 379–387.
- RUDELS, B. 1987. On the mass balance of the Polar Oceans, with special emphasis on the Fram Strait. *Nor. Polarinst. Skr.* **188**: 1–53.
- , L. G. ANDERSON, AND E. P. JONES. 1996. Formation and evolution of the surface mixed layer and halocline of the Arctic Ocean. *J. Geophys. Res.* **101**: 8807–8821.
- , E. P. JONES, L. G. ANDERSON, AND G. KATTNER. 1994. On the intermediate depth waters of the Arctic Ocean, p. 33–46. *In* O. M. Johannessen, R. D. Muench, and J. E. Overland [eds.], *The polar oceans and their role in shaping the global environment*. Am. Geophys. Union.
- RYTHER, J. G., AND W. M. DUNSTAN. 1971. Nitrogen, phosphorous, and eutrophication in the coastal marine environment. *Science* **171**: 1008–1013.
- SAKSHAUG, E., AND H. R. SKJOLDAL. 1989. Life at the ice edge. *Ambio* **18**: 60–67.
- SAMBROTTO, R. N., AND OTHERS. 1993. Elevated consumption of carbon relative to nitrogen in the surface ocean. *Nature* **363**: 248–250.
- SARMIENTO, J. L., AND J. R. TOGGWEILER. 1984. A new model for the role of the oceans in determining atmospheric pCO<sub>2</sub>. *Nature* **308**: 621–624.
- SCHAUER, U., R. MUENCH, B. RUDELS, AND L. TIMOKHOV. 1997. The impact of eastern Arctic Shelf waters on the Nansen Basin intermediate layers. *J. Geophys. Res.* **102**: 3371–3382.
- SCHLOSSER, P., D. BAUCH, R. FAIRBANKS, AND G. BÖNISCH. 1994. Arctic river-runoff: Mean residence time on the shelves and in the halocline. *Deep-Sea Res.* **41**: 1053–1068.
- SCRIPPS INSTITUTE OF OCEANOGRAPHY. 1984. Data report, C.S.S., Hudson cruise 82–001, 14 February–6 April 1982, 1. Physical and chemical data, SIO Ref. 84–14. Univ. of California, La Jolla.
- SHAFFER, G. 1996. Biogeochemical cycling in the global ocean 2. New production, Redfield ratios, and remineralization in the organic pump. *J. Geophys. Res.* **101**: 3723–3745.
- SLAGSTAD, D., AND P. WASSMANN. 1996. Climate change and carbon flux in the Barents Sea: 3-D simulations of ice-distribution, primary production and vertical export of particulate organic carbon. *Mem. Nat. Inst. Polar Res.* **51**: 119–141.
- SMETHIE, W. M., JR., D. W. CHIPMAN, J. H. SWIFT, AND K. P. KOLTERMANN. 1988. Chlorofluorocarbons in the Mediterranean Seas: Evidence for formation of bottom water in the Eurasian Basin and deep water exchange through Fram strait. *Deep-Sea Res.* **35**: 347–369.
- SPRINGER A. M., AND C. P. MCROY. 1993. The paradox of pelagic food webs in the northern Bering Sea—III. Patterns of primary production. *Cont. Shelf Res.* **13**: 575–600.
- STEEL, M., J. H. MORRISON, AND T. B. CURTIN. 1995. Halocline water formation in the Barents Sea. *J. Geophys. Res.* **100**: 881–894.
- SUBBA RAO, D. V., AND T. PLATT. 1984. Primary production of Arctic waters. *Polar Biol.* **3**: 191–201.
- TAKAHASHI, T., J. OLAFSON, J. G. GODDARD, D. W. CHIPMAN, AND S. C. SUTHERLAND. 1993. Seasonal variation of CO<sub>2</sub> and nutrients in the high-latitude surface oceans: A comparative study. *Global Biogeochem. Cycles* **7**: 843–878.
- TELANG, S. A., R. POCKLINGTON, A. S. NAIDU, E. A. ROMANKEVICH, I. I. GITELSON AND M. I. GLADYSHEV. 1991. Carbon and mineral transport in major North American, Russian Arctic, and Siberian Rivers: The St. Lawrence, the Mackenzie, the Yukon, the Arctic Alaskan Rivers, the Arctic Basin Rivers in the Soviet Union, and the Yenisei, p. 75–104. *In* E. T. Degens, S. Kempe, and J. E. Richey [eds.], *Biogeochemistry of major world rivers*. Wiley.
- UNTERSTEINER, N. 1986. Types of ice, p. 5–29. *In* N. Untersteiner [ed.], *The geophysics of sea ice*, chapter 2, series B, Physics. NATO ASI Series.
- WALLACE D. W. R., P. J. MINNETT, AND T. S. HOPKINS. 1995. Nutrients, oxygen, and inferred new production in the northeast water polynya, 1992. *J. Geophys. Res.* **100**: 4323–4340.
- , P. SCHLOSSER, M. KRYSELL, AND G. BÖNISCH. 1992. Halocarbon ratio and tritium/<sup>3</sup>He dating of water masses in the Nansen Basin, Arctic Ocean. *Deep-Sea Res.* **39**: S435–S458.
- WALSH, J. J., AND OTHERS. 1989. Carbon and nitrogen cycling within the Bering/Chukchi seas: Source region for organic matter effecting AOU demand of the Arctic Ocean. *Prog. Oceanogr.* **22**: 277–359.
- WHEELER, P. A., M. GOSSELIN, E. SHERR, D. THIBAUT, D. L. KIRCHMAN, R. BENNER, AND T. E. WHITLEDGE. 1996. Active cycling of organic carbon in the central Arctic Ocean. *Nature* **380**: 697–699.
- WILSON, C., AND D. W. R. WALLACE. 1990. Using the nutrient ratio NO/PO as a tracer of continental shelf water in the central Arctic Ocean. *J. Geophys. Res.* **95**: 22193–22208.
- YAGER, P. L., D. W. R. WALLACE, K. M. JOHNSON, W. O. SMITH, JR., P. J. MINNETT, AND J. W. DEMING. 1995. The northeast water polynya as an atmospheric CO<sub>2</sub> sink: A seasonal rectification hypothesis. *J. Geophys. Res.* **100**: 4389–4398.

Received: 17 April 1997

Accepted: 16 January 1998